chemistry proceedings

MDPI

Proceedings

Structural Investigation of the Carbon Deposits on Ni/Al_2O_3 Catalyst Modified by CaO-MgO for the Biogas Dry Reforming Reaction †

Nikolaos D. Charisiou [1], Georgios I. Siakavelas [1], Victor Sebastian [2], Steven J. Hinder [3], Mark A. Baker [3], Vagelis G. Papadakis [4], Wen Wang [5], Kyriaki Polychronopoulou [6,7] and Maria A. Goula [1,*]

[1] Laboratory of Alternative Fuels and Environmental Catalysis (LAFEC), Department of Chemical Engineering, University of Western Macedonia, 50100 Kozani, Greece; ncharisiou@uowm.gr (N.D.C.); giorgosiakavelas@gmail.com (G.I.S.)
[2] Chemical and Environmental Engineering Department, Instituto de Nanociencia de Aragón (INA) and Instituto de Ciencia de Materiales de Aragón (ICMA), Universidad de Zaragoza-CSIC, 50018 Zaragoza, Spain; victorse@unizar.es
[3] The Surface Analysis Laboratory, Faculty of Engineering and Physical Sciences, University of Surrey, Guildford GU2 4DL, UK; s.hinder@surrey.ac.uk (S.J.H.); m.baker@surrey.ac.uk (M.A.B.)
[4] Department of Environmental Engineering, University of Patras, 30100 Agrinio, Greece; vgpapadakis@upatras.gr
[5] Biomass Energy and Environmental Engineering Research Center, Beijing University of Chemical Technology, Beijing 100029, China; wangwen@mail.buct.edu.cn
[6] Center for Catalysis and Separation, Khalifa University of Science and Technology, Abu Dhabi, P.O. Box 127788, UAE; kyriaki.polychrono@ku.ac.ae
[7] Department of Mechanical Engineering, Khalifa University of Science and Technology, Abu Dhabi, P.O. Box 127788, UAE
* Correspondence: mgoula@uowm.gr
† Presented at the 1st International Electronic Conference on Catalysis Sciences, 10–30 November 2020; Available online: https://eccs2020.sciforum.net.

Published: 9 November 2020

Abstract: Ni catalysts based on Al_2O_3 and Al_2O_3 modified with CaO-MgO were tested for the dry reforming of biogas (BDR). Time-on-stream experiments were carried out between 600 and 800 °C, and the spent catalysts were examined using a variety of characterization techniques including, N_2 adsorption/desorption, thermogravimetric analysis (TGA), Raman spectroscopy, electron microscopy (STEM-HAADF and HR-TEM), and X-ray photoelectron spectroscopy (XPS). It was revealed that the carbon deposits consisted of carbon nanotubes and amorphous carbon for both samples. XPS studies showed the presence of Ni^0 on both catalysts and $Ni_2O_3/NiAl_2O_4$ on the Ni/Al_2O_3 sample. The time-on-stream experiments showed that the $Ni/CaO\text{-}MgO\text{-}Al_2O_3$ catalyst is more resistant to deactivation and more active and selective for all temperatures under investigation. It was concluded that doping Al_2O_3 with CaO-MgO enhances catalytic performance as: (a) it helps to maintain highly dispersed Ni^0 during the BDR as the interaction between metal and support is a stronger one, (b) it leads to the formation of carbon structures that are easier to oxidize, and (c) it facilitates the gasification of the carbon deposits because its increased surface basic sites enhance the adsorption of carbon dioxide.

Keywords: biogas dry reforming; syngas production; nickel-based catalysts; catalytic deactivation; carbon deposition; CaO-MgO modifiers

1. Introduction

Biogas is a product of the anaerobic digestion of biomass. It contains mainly CH_4 and CO_2 and can be used for the production of syngas (H_2/CO) via dry reforming (BDR) [1]. Syngas is a valuable feedstock in the chemical industry used for the synthesis of oxygenated chemicals and hydrocarbons via the Fisher–Tropsch process [2]. The major issue that must be overcome when using cheap Ni based systems is carbon deposition on the catalyst surface, which is produced via methane decomposition and carbon monoxide disproportionation. The carbon deposited on the catalyst surface can differ in nature and structure [3–5]. As is widely understood, the activity of a catalyst system depends on a number of factors, which include the nature of the support and active metal, the catalyst preparation method, and pretreatment. Popular metal oxides tested as supports for Ni based catalysts include Al_2O_3, SiO_2, ZrO_2, rare earth metals (e.g., La_2O_3 and CeO_2) [6–9], or alkaline earth metals (e.g., Ba, Ca, Sr) [10–12] as promoters. The present work reports on the catalytic performance of Ni/Al and Ni/CaO-MgO-Al (Ni/modAl) catalysts using typical biogas mixtures (CH_4/CO_2 = 1.5). It examines the amount and/or the quality of deposited carbon after the time-on-stream experiments and relates this with catalyst deactivation. To achieve this aim, the time-on-stream experiments were performed at different reaction temperatures and the carbon deposited on the spent catalysts was examined by various characterization techniques (N_2 adsorption/desorption, TGA, Raman, STEM-HAADF, HR-TEM, and XPS). The evolution of Ni oxidation states during the reaction was investigated using XPS.

2. Materials and Methods

2.1. Catalyst Preparation

The alumina support was obtained from Akzo and the modified alumina (4.5% CaO, 1% MgO, 0.5% SiO_2) by Saint Gobain NorPro in pellet form. The supports were crashed and sieved to 350–500 μm and calcined at 800 °C for 4 h. The catalysts were prepared via the wet impregnation technique using the appropriate $Ni(NO_3)_2$ $6H_2O$ solution to give catalysts with a Ni content of 8 wt.%. The catalysts were dried at 120 °C for 12 h, calcined in atmosphere at 800 °C for 4 h, and in situ activated for 1 h at 800 °C under pure H_2 flow. The catalysts are denoted as Ni/Al and Ni/modAl.

2.2. Materials Characterization

The spent catalysts were examined using the following instruments/techniques: (a) Leco TGA 701, (b) S-Twin Tecnai (200 kV G2 20) and Tecnai G2-F30 Field Emission Gun microscope (STEM-HAADF and HR-TEM), (c) ThermoFisher Scientific Instruments K-Alpha+ spectrometer (XPS), (d) WITEC alpha 300R micro-Raman system, and (e) high-resolution 3Flex Micromeritics porosimeter (N_2 adsorption/desorption).

2.3. Catalysts Tests

The experimental apparatus used was a continuous flow fixed bed tubular reactor. The tests were carried out at atmospheric pressure. The gas mixture fed into the system was 55% CH_4, 35% CO_2, and 10% Ar (CH_4/CO_2 molar ratio = 1.57). Short (10 h) time-on-stream experiments were carried out at different temperatures. The weight hourly space velocity (WHSV) was 40,000 mL g^{-1} h^{-1}. The analysis of the reactants and products was carried out by gas chromatography in a CG-Agilent 7890A.

3. Results and Discussion

3.1. Characterization of Spent Catalysts

3.1.1. Textural Characterization

The N_2 adsorption/desorption isotherms for the Ni/Al and Ni/modAl catalysts after their in situ reduction and after reaction at 600, 700, and 800 °C are presented in Figure 1. The respective pore size

distribution curves are also presented as insets on the corresponding figures. The isotherms for both samples are type IVa. The hysteresis loop for the reduced Ni/Al sample is type H2(b) (typical of mesoporous materials), but after reaction, this loop is transformed to an H3 type (usually found in materials with macropores). Regarding the Ni/modAl samples, the hysteresis loop is H3 type. This is because, although the adsorption branch resembles a Type II isotherm, the lower limit of the desorption branch is located at the cavitation-induced P/P_0.

Regarding the pore size distribution, for the Ni/Al samples, these are single modal types in the mesopore range, centered around 10–20 nm. However, a shift to the micropore range is observed for the samples used at 600 and 700 °C. This is opposing to what can be concluded for the Ni/modal samples, which show that the majority of the population of pores is in the meso-range. Additionally noticeable for the spent catalysts is a shift to a bigger mean diameter, which provides an indication that pore blogging occurs at the meso-range. It can be deduced that for both spent catalysts, the carbon deposition that took place at lower reaction temperatures (600 and 700 °C) covered the mesopores.

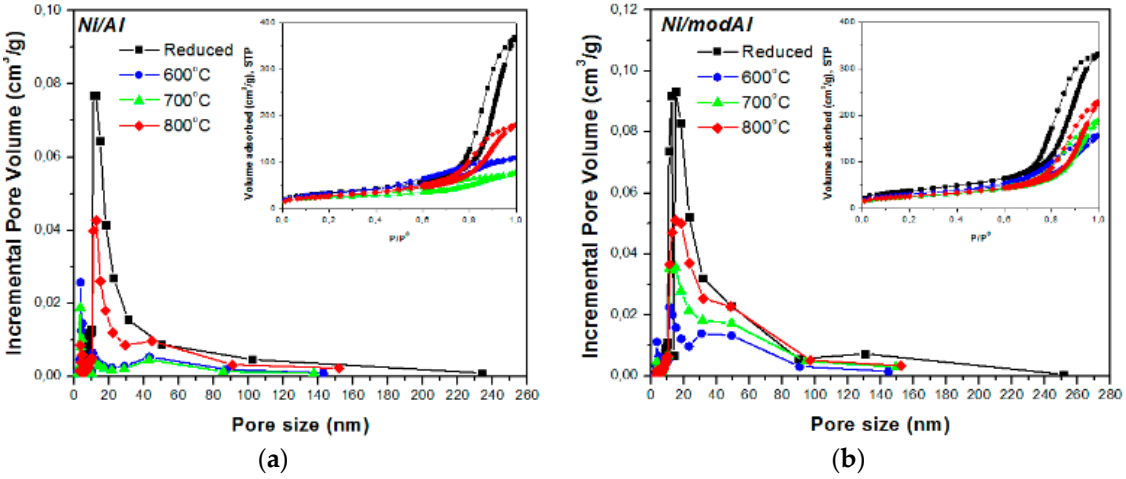

(**a**) (**b**)

Figure 1. Pore size distribution and N_2 adsorption–desorption isotherms (inset) of the reduced and spent (**a**) Ni/Al and (**b**) Ni/modAl catalysts at 600, 700, and 800 °C.

3.1.2. TGA Analysis

From the TGA analysis (not shown herein), it was observed that the oxidation process was different between the two catalysts. For the Ni/Al, the main thermal event was found between ≈450–700 °C for the samples tested at low reaction temperatures (600 and 650 °C), but it included up to 800 °C for the catalysts tested at higher reaction Ts. In contrast, for the Ni/modAl, the main thermal event was ≈450–800 °C. According to the literature, amorphous carbon combusts between 200–500 °C, carbon nanofibers (CNFs) and/or carbon nanotubes (CNTs) combust between 500–600 °C, and more graphitic structures, such as multi wall carbon nanotubes (MWCNTs), combust between 600–800 °C [13]. Although these results show that different carbon structures were deposited on the catalysts during the reaction, it appears that a bigger fraction of graphitic coke was deposited on the Ni/Al, especially at higher reaction temperatures. Thus, it can be concluded that the addition of MgO and CaO on the alumina supporting material led to a less graphitic type of carbon, due to the higher rate of carbon oxidation, which could lead to a catalyst with improved stability characteristics.

3.1.3. Raman Spectroscopy Analysis

The results obtained using Raman spectroscopy are shown in Figure 2. This technique allows the investigation of the nature (graphitization) of the carbon deposits. Both samples show peaks between 1000 and 2000 cm^{-1} (first order region) and between 2300 and 3300 cm^{-1} (second order region). In the first order region are located two broad bands; these are termed the G-band (between 1500 and 1600 cm^{-1}) and D-band (between 1300 and 1400 cm^{-1}). Deconvolution of the Raman spectra

showed that the G and D-band peaks were centered at 1565 and 1345 cm^{-1} corresponding to CNTs. The extent of graphitization of the coke can be gauged by the relative intensity of the D and G-bands (I_D/I_G), namely lower I_D/I_G values are correlated with higher crystallinity due to the higher contribution of the G-band [14]. For all catalysts tested for the present work, it is obvious that the degree of crystallinity increased with an increase in the reaction temperature; however, this increase was more significant for the unmodified nickel catalyst. To illustrate the point, the I_D/I_G ratio for the Ni/Al sample followed the order 1.32 > 0.72 > 0.45 > 0.44 > 0.35 and for the modified catalyst 1.42 > 1.18 > 1.06 > 0.98 > 0.86 at 600, 650, 700, 750, and 800 °C, respectively.

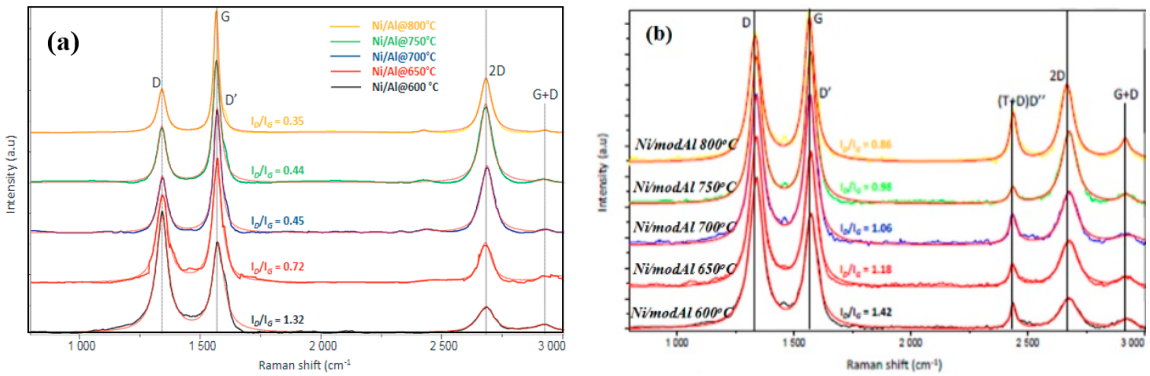

Figure 2. Raman spectra of spent (**a**) Ni/Al and (**b**) Ni/modAl catalysts.

3.1.4. Electron Microscopy Analysis

At 600 °C, both samples exhibited crystalline carbon allotropes shaped as carbon nanotubes and amorphous carbon; coke encapsulating Ni particles can also be observed. In contrast, at high reaction temperatures (800 °C), no amorphous carbon was detected on the Ni/Al catalyst; only coke encapsulating the active metallic Ni nanoparticles (NPs) could be observed. This was in contrast to the conclusion drawn regarding the Ni/modAl spent catalyst, where amorphous carbon could be observed even after reaction at 800 °C [15]. Another interesting observation was that at 800 °C the Ni/Al catalyst showed the formation of core-shell carbon coated Ni NPs with highly graphitized CNTs formed. This provides a good explanation for the very low I_D/I_G ratios discussed above. From HR-TEM, a plethora of defects on the CNTs formed onto the Ni/modAl system could be observed. These defects can be explained by the transfer of oxygen and its insertion in the graphitic lattice during CNT growth, which inhibits the formation of CNTs with continuous, straight walls.

3.2. Catalytic Stability

As mentioned above, time-on-stream experiments for the Ni/Al and Ni/modAl were carried out at a variety of reaction temperatures (600, 650, 700, 750, 800 °C). To allow fair comparison, a fresh catalytic sample was used for each experiment. The changes regarding XCH_4, XCO_2, and YH_2 during BDR are depicted in Figure 3. The Ni/Al catalyst shows a steep drop in the conversion and yield values during the first two hours of the reaction (except at 800 °C), which leads to the loss of approximately half of its activity. In contrast, it is obvious that the Ni/modAl catalyst is more stable, active, and selective. These differences are less pronounced at high reaction temperature. As an example, at 650 °C, the Ni/modAl presents almost double the values for XCH_4 (40%) and YH_2 (35%) over the Ni/Al.

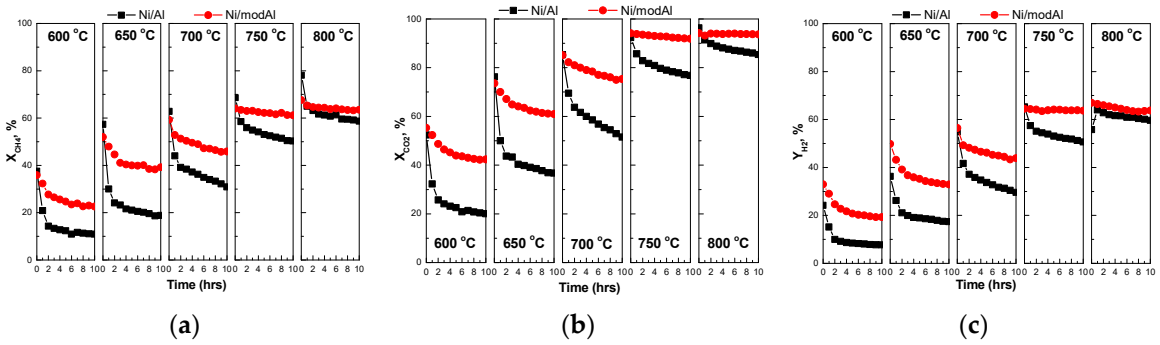

Figure 3. (**a**) CH_4 and (**b**) CO_2 conversion (%) and (**c**) H_2 yield (%) for the Ni/Al and Ni/modAl catalysts for stability tests conducted at different temperatures.

Another observation is that for both catalysts the loss in activity loss decreases as test are carried out at higher reaction temperature. To be more specific, for the Ni/Al sample, the activity loss ($\Delta X(CH_4)$%) is between 70% (600 °C) and 20% (800 °C), and for the Ni/modal, it is between 50% (600 °C) and ≈5% (800 °C). It is pointed out that XCO_2, YH_2, and YCO are affected by the reverse water gas shift (RWGS) reaction, and only the XCH_4 provides a true indication of the DRM activity.

Finally, regarding the H_2/CO molar ratio, its values are almost constant for the duration of the time-on-stream tests except for the first 2 h of operation in which elevated H_2/CO values (up to 1) were recorded. The high H_2/CO values point to a significant occurrence of the CH_4 cracking reaction, and/or Boudouard reaction. These reactions are mainly responsible for carbon deposition. The severe deactivation shown by both catalysts is also due to the harsh experimental conditions used in this study, i.e., the gas mixture used as feed had a high CH_4 to CO_2 ratio (equal to 1.57) and was almost undiluted.

4. Conclusions

In the present work, the time-on-stream stability of Ni/Al and Ni/modAl catalysts was examined for the reaction of the dry reforming of biogas. The study focused on the correlation between deactivation and carbon deposition. In particular, for both spent catalysts, TGA and Raman results proved that the degree of coke graphitization increased with higher reaction temperatures. The use of CaO and MgO as modifiers helped obtain coke deposits that were less graphitic in type. The TEM analysis showed that both catalysts contained graphitic structures in the shape of carbon nanotubes and co-existent amorphous carbon. The HR-TEM images showed in a clear manner the defects of the CNTs formed onto the spent Ni/modAl catalyst. The time-on-stream tests showed that deactivation for the modified catalyst was less pronounced for all reaction temperatures. Thus, the modification of Al_2O_3 with CaO and MgO helped maintain the Ni^0 phase during the reaction (due to stronger active phase-support interactions) and improved the deposited carbon gasification via the reverse Boudouard reaction. The latter was achieved by an enhancement of CO_2 adsorption on the catalyst's increased surface basic sites.

Author Contributions: Conceptualization, N.D.C.; data curation, G.I.S., V.S., S.J.H., V.G.P., W.W.; formal analysis, N.D.C., G.I.S., M.A.B., K.P.; funding acquisition, M.A.G., V.G.P., W.W.; methodology, N.D.C.; project administration, N.D.C., M.A.G.; project coordination, M.A.G.; resources, M.A.G.; supervision, N.D.C.; writing—original draft, G.I.S.; writing—review and editing, N.D.C., M.A.B., K.P., M.A.G. All authors have read and agreed to the published version of the manuscript.

Acknowledgments: This research has been co-financed by the European Union and Greek national funds under the call "Greece—China Call for Proposals for Joint RT&D Projects" (Project code: T7DKI-00388).

Conflicts of Interest: The authors declare no conflict of interest.

References

1. Goula, M.A.; Charisiou, N.D.; Papageridis, K.N.; Delimitis, A.; Pachatouridou, E.; Iliopoulou, E.F. Nickel on alumina catalysts for the production of hydrogen rich mixtures via the biogas dry reforming reaction: Influence of the synthesis method. *Int. J. Hydrogen Energy* **2015**, *40*, 9183–9200.
2. Charisiou, N.D.; Siakavelas, G.; Papageridis, K.N.; Baklavaridis, A.; Tzounis, L.; Avraam, D.G.; Goula, M.A. Syngas production via the biogas dry reforming reaction over nickel supported on modified with CeO_2 and/or La_2O_3 alumina catalysts. *J. Nat. Gas Sci. Eng.* **2016**, *31*, 164–183.
3. Goula, M.A.; Charisiou, N.D.; Siakavelas, G.; Tzounis, L.; Tsiaoussis, I.; Panagiotopoulou, P.; Goula, G.; Yentekakis, I.V. Syngas production via the biogas dry reforming reaction over Ni supported on zirconia modified with CeO_2 or La_2O_3 catalysts. *Int. J. Hydrogen Energy* **2017**, *42*, 13724–13740.
4. Italiano, C.; Balzarotti, R.; Vita, A.; Latorrata, S.; Fabiano, C.; Pino, L.; Cristiani, C. Preparation of structured catalysts with Ni and Ni-Rh/CeO_2 catalytic layers for syngas production by biogas reforming processes. *Catal. Today* **2016**, *273*, 3–11.
5. Juan-Juan, J.; Roman-Martinez, M.C.; Illan-Gomez, M.J. Nickel catalyst activation in the carbon dioxide reforming of methane: Effect of pretreatments. *Appl. Catal. A-Gen.* **2009**, *355*, 27–32.
6. Montoya, J.A.; Romero-Pascual, E.; Gimon, C.; Del Angel, P.; Monzon, A. Methane reforming with CO_2 over Ni/ZrO_2-CeO_2 catalysts prepared by sol-gel. *Catal. Today* **2000**, *63*, 71–85.
7. Zhan, Y.; Han, J.; Bao, Z.; Cao, B.; Li, Y.; Street, J.; Yu, F. Recent advances in dry reforming of methane over Ni-based catalysts. *Mol. Catal.* **2017**, *436*, 248–258.
8. Kathiraser, Y.; Wang, Z.; Ang, M.L.; Mo, L.; Li, Z.; Oemar, U.; Kawi, S. Highly active and coke resistant Ni/SiO_2 catalysts for oxidative reforming of model biogas: Effect of low ceria loading. *J. CO_2 Util.* **2017**, *19*, 284–295.
9. Vasiliades, M.A.; Makri, M.M.; Djinovic, P.; Erjavec, B.; Pintar, A.; Efstathiou, A.M. Dry reforming of methane over 5wt% Ni/$Ce_{1-x}Pr_xO_{2-\delta}$ catalysts: Performance and characterisation of active and inactive carbon by transient isotopic techniques. *Appl. Catal. B-Environ.* **2016**, *197*, 168–183.
10. Bellido, J.D.A.; Assaf, E.M. Effect of the Y_2O_3-ZrO_2 support composition on nickel catalyst evaluated in dry reforming of methane. *Appl. Catal. A-Gen.* **2009**, *352*, 179–187.
11. Rezaei, M.; Alavi, S.M.; Sahebdelfar, S.; Yan, Z.-F. Effects of K_2O promoter on the activity and stability of nickel catalysts supported on mesoporous nanocrystalline zirconia in CH_4 reforming with CO_2. *Energy Fuel* **2008**, *22*, 2195–2202.
12. Charisiou, N.D.; Papageridis, K.N.; Tzounis, L.; Sebastian, V.; Baker, M.A.; Hinder, S.J.; AlKetbi, M.; Polychronopoulou, K.; Goula, M.A. Ni supported on CaO-MgO-Al_2O_3 as a highly selective and stable catalyst for H_2 production via the glycerol steam reforming reaction. *Int. J. Hydrogen Energy* **2019**, *44*, 256–273.
13. Velasquez, M.; Batiot-Dupeyrat, C.; Gallego, L.; Santamaria, A. Chemical and morphological characterization of multi-walled-carbon nanotubes synthesized by carbon deposition from an ethanol-glycerol blend. *Diam. Relat. Mater.* **2014**, *50*, 38–48.
14. Awadallah, A.E.; Aboul-Enein, A.A.; El-Desouki, D.S.; Aboul-Gheit, A.K. Catalytic thermal decomposition of methane to COx-free hydrogen and carbon nanotubes over MgO supported bimetallic group VIII catalysts. *Appl. Surf. Sci.* **2014**, *296*, 100–107.
15. Sutthiumporn, K.; Kawi, S. Promotional effect of alkaline earth over Ni-La_2O_3 catalyst for CO_2 reforming of CH_4: Role of surface oxygen species on H_2 production and carbon suppression. *Int. J. Hydrogen Energy* **2011**, *36*, 14435–14446.